Superconductive Digital Instantaneous Frequency Measurement Subsystem

Guo-chun Liang, *Member, IEEE,* Chien-Fu Shih, Richard S. Withers *Member, IEEE,* Brady F. Cole, Marie E. Johansson, and Larry P. Suppan, Jr.

***Abstract*—A five bit high-temperature superconductive digital instantaneous frequency measurement (DIFM) subsystem has been constructed for the determination of the frequency of unknown signals over a 500 MHz bandwidth, centered on 4 GHz, with a resolution of ±7.8 MHz. The subsystem contains a cryogenic section with five discriminator modules utilizing superconductive delay lines, GaAs mixers, and power dividers. The subsystem also has a room temperature GaAs limiting amplifier and a silicon postprocessor. With a single tone CW input between −40 dBm and +10 dBm, the frequency quantization boundaries of the subsystem are, on average, 3.1 MHz from their design values. This system demonstrates the potential system level application of high-temperature superconductive electronics in instrumentation, communication, radar, and electronic warfare.**

I. Introduction

THE discovery of high-temperature superconductors (HTS) has fundamentally changed the prospects of superconductive electronics. The low surface resistance of superconducting materials makes possible microwave devices and circuits with very high Q, low insertion loss, and low dispersion. Various devices, such as resonators, delay lines, filters, couplers, and antennas, have been demonstrated. In this paper, we report a digital IFM subsystem, which is one of the first demonstrations of superconductive electronics at the subsystem level.

Instantaneous frequency measurement (IFM) subsystems are widely used in electronic warfare (EW) and electronic intelligence (ELINT) systems for the determination of the frequency of unknown signals over a broad frequency band [1]. They perform this function by the comparison of the phase of the unknown signal with the phase of a time delayed replica of it. In order to perform this function accurately, wideband long microwave delay lines are important. The accuracy of the reported frequency in DIFM systems is largely dependent on the length and fidelity (i.e., phase accuracy) of these delay lines.

For communication and surveillance applications, scanning superheterodyne receivers have the advantage of distinguishing simultaneous emitters and the capability to extract data from a given carrier. However, scanning receivers have a small instantaneous bandwidth or, equivalently, a small probability of intercept (POI). An IFM, on the other hand, is sensitive at all times to its entire bandwidth, and can be used to cue the scanning receiver to the frequency of a detected emitter.

Channelized receivers, consisting of a bank of narrowband filters with contiguous bands, have a higher probability of intercept than scanning receivers because of their high degree of parallelism. This parallelism, however, comes at the price of size, weight, and possibly power. Practical considerations make it difficult to cover wide bands with high POI. The use of an IFM to cue the filter bank to bands with activity can significantly enhance the system effectiveness.

In summary, IFM systems have moderately high sensitivity, high dynamic range, excellent frequency accuracy, high POI, and broad instantaneous bandwidth [2]–[3].

Conventional DIFM systems use delay lines made by coiling coaxial cables or (for shorter delay) by patterning meander lines of normal metal microstrip. However, the loss and bulk of these approaches limit the amount of available delay. In order to recover sufficient frequency resolution with short delay lines, system designers are forced to use more accurate phase detection schemes, placing demands on the mixers, phase shifters, and baseband circuitry used in the phase detectors [4]. Superconductive delay lines offer the highest bandwidth with lowest loss and dispersion compared to currently available technology. Long, low-loss, broadband superconductive delay lines permit the use of simple binary phase detection for frequency determination.

One intrinsic limitation of IFM systems is that only one tone can be measured at a given instant, and other spectral components may degrade the measurement. We report here the two tone performance of the HTS DIFM subsystem.

II. Architecture of the DIFM Subsystem

The architecture of the present DIFM subsystem is shown in Fig. 1(a). The incoming IF signal is split by a 5-way power divider to feed five phase discrimination channels, each of which provides one bit of the frequency word. In each channel, the power is further split into two paths, one of which is applied directly to the LO port of the correlation mixer while the other is routed through a delay line, the output of which is fed to the mixer RF port.

Manuscript received April 4, 1993; revised June 14, 1993. This work was sponsored by the U.S. Naval Research Laboratory.

The authors are with Conductus, Inc., Sunnyvale, CA 94086.

IEEE Log Number 9212952.

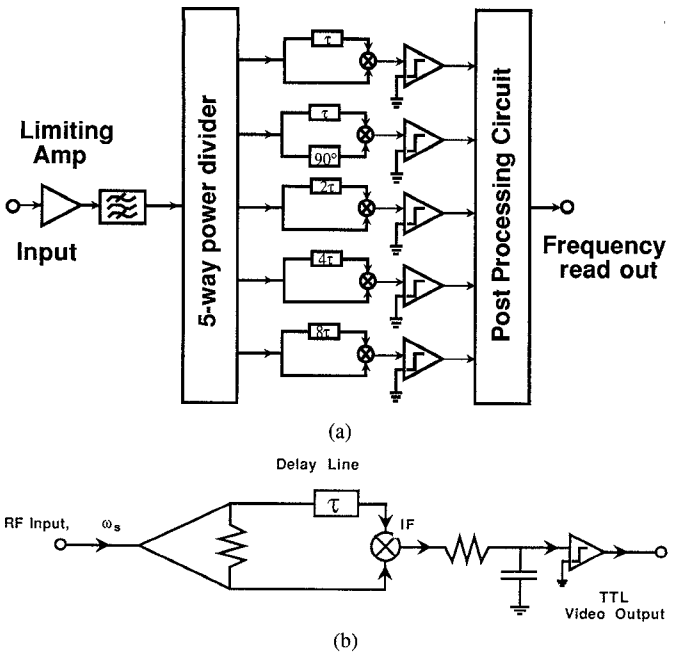

Fig. 1. (a) Schematic diagram of the DIFM subsystem. (b) Schematic diagram of the DIFM phase discriminator.

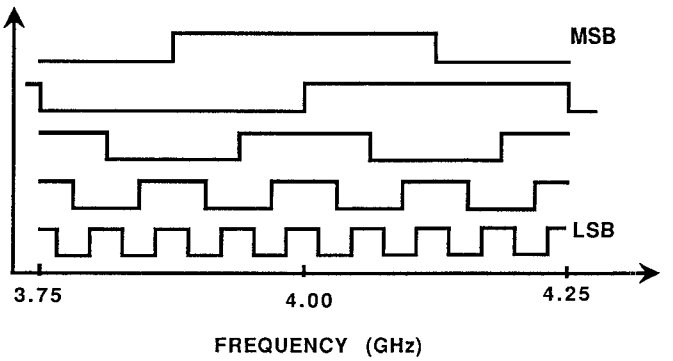

Fig. 2. Ideal DIFM digital output waveform. 2 ns (in phase) 2 ns (quadrature), 4-ns, 8-ns, and 16-ns channels are arranged from top to bottom.

The phase correlation is obtained by lowpass filtering the output of the mixer. This baseband output is then hard limited to obtain the appropriate bit of the binary representation of the input signal frequency.

The delay in successive channels of the DIFM is stepped by factors of two, with the exception of the two most significant bits (MSBs), which are the same length but with a 90-degree phase difference. This configuration produces a Gray code, which is then converted to natural binary code, and then to decimal form. The processing time needed to accomplish this measurement, and hence the minimum length pulses which can be processed, is on the order of the time delay of the least significant bit (LSB) discriminator. The time delay associated with the LSB discriminator of a DIFM that uses a set of basic cosine binary correlators is given by $t_d = 1/4f_r$, where f_r is the desired frequency resolution.

The key elements in the subsystem are the delay lines and the phase comparators. The resolution of the frequency determination is dependent on the length of the delay line; it is $\pm(8\ \tau_{\max})^{-1}$ where $\tau_{\max}$ is the length of the longest delay. In our subsystem, the longest line is 16 ns, giving a resolution of ± 7.8 MHz. (Resolution may also be enhanced by performing multibit phase measurements on the output of the branch with the longest delay.) It is very important that deviations from linear phase (constant group delay) be minimized in these delay lines, as such deviations result directly in errors in the frequencies at which the output bits switch. It is also critical that the line lengths be accurately controlled.

As shown in Fig. 1(a), a DIFM subsystem uses a bank of frequency discriminators with the longest delay corresponding to the desired frequency resolution, while the shortest delay is determined by the bandwidth to be measured. The discriminator of the DIFM receiver shown in Fig. 1(b) provides IF voltages equal to $\cos \omega_s \tau_d$. Processing $\cos \omega_s \tau_d$ through a binary comparator produces an output with transitions at $\omega_n = (n + 1/2)\pi/\tau_d$. A set of m correlators with binary outputs can divide the unambiguous frequency range corresponding to the shortest delay correlator into 2^m frequency cells. In our design, we chose the frequency range of 3.75–4.25 GHz. We use 5 delay lines having delays of 16 ns, 8 ns, 4 ns, 2 ns, and 2 ns, respectively. Fig. 2 shows the ideal output waveforms of that system.

It is clear from Fig. 2 that the performance of the system is fully characterized by the ω_n at which the transitions between frequency bins occur. As stated above, these transition frequencies should be at $f_n = (n + 1/2)/2\tau_d$. The deviations of the measured transition frequencies from this design value are important performance measures.

Fig. 3 shows the predicted standard deviation of the transition frequency as a function of input frequency, if there were such variations in delay line length. All five delay lines have Gaussian distributed errors about their nominal design values with standard deviations of 1, 5, and 10 ps. In the simulation, the quantization error is not included. As we can see, the deviations due to shorter delay lines create larger deviations in transition frequencies and the deviations of the transition frequencies due to a particular delay line increase with the input frequency. As expected larger errors in delay line lengths cause larger errors in transition frequencies. The requirement on the precision of the delay line length will become tighter if the quantization is made smaller (i.e., longer delay lines are used).

An important issue associated with the phase discriminator is an accurate zero reference to ensure that switching occurs at designed frequency value. Otherwise, errors in the reported frequency occur. This possible offset could be caused by imbalance and phase errors in the RF circuitry and by lack of matching of diode characteristics. A performance analysis has been done for variations in the zero reference of the comparator. In the analysis, it is assumed that a limiting amplifier is used in front of the DIFM cryogenic section so that the input signal (and, in

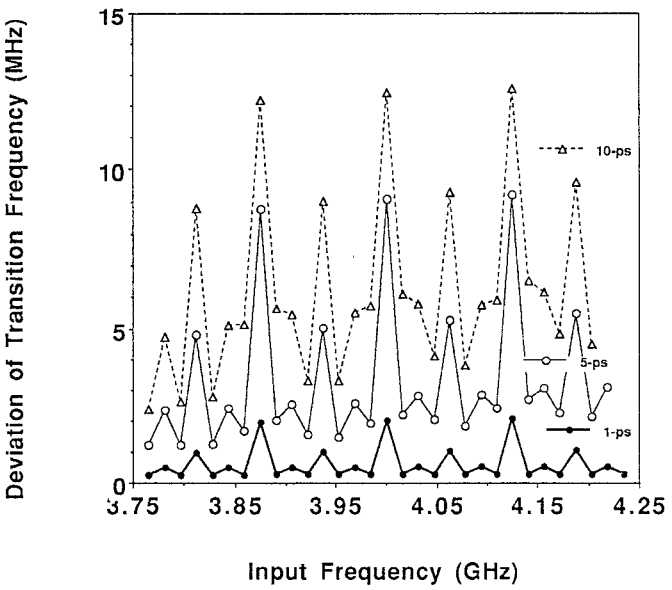

Fig. 3. Standard deviation of the transition frequency error versus design frequency calculated from assumed delay-line length variations. Each delay line is assumed to have an independent Gaussian distributed delay error about its nominal delay value with a deviation of 1 ps (bottom curve), 5 ps (middle curve), and 10 ps (top curve).

turn, the outputs of the mixer) are of constant magnitude. If there is no error, the frequency readout error is no more than quantization error. But if there is a Gaussian distributed zero reference error in the five channels with an rms value of 10% of the mixer output magnitude, the frequency readout error is just slightly more severe than the quantization error. Finer quantization, of course, will tighten this rather loose requirement.

III. Implementation of the DIFM

The system utilizes HTS material. The delay lines are made from $YBa_2Cu_3O_{7-\delta}$ (YBCO) on 20-mil-thick $LaAlO_3$ substrates in a stripline configuration. The other circuits are made on M-plane sapphire in a microstrip configuration. We have used modified Wilkinson power dividers to split the incoming signal into five paths. The phase detection mixers use GaAs diodes. To reduce the operational power level and thermal load, we use low-barrier-height Schottky diodes as mixing diodes at 77 K. We utilized silicon comparators and encoders for postprocessing. Key components are discussed further below.

A. Limiting Amplifier

The limiting amplifier, with a bandpass filter, is used to increase the sensitivity and clean up the signal within the band of interest. The limiting amplifier has the advantage of reducing the discriminator output sensitivity to variations in the signal level, thus improving frequency accuracy. The limiting process also reduces the effects of simultaneous input tones because of the well known small signal suppression effect of limiters. The sensitivity of an IFM receiver with a limiting amplifier is primarily determined by the noise figure of the limiting amplifier.

We have used a five stage GaAsFET amplifier which has an input power range from −40 dBm to +10 dBm and output power of 16 dBm. With the output filter, the suppression of adjacent harmonics is over 35 dB.

B. Delay Lines

The bandwidth, resolution, accuracy, and sensitivity of the IFM subsystem are largely determined by the length and quality of the delay lines. Common devices of this type include normal metal electromagnetic delay lines, surface acoustic wave (SAW) devices, and bulk ultrasonic delay lines. Compared to these delay lines, superconductive delay lines offer the highest bandwidth with the lowest loss and dispersion.

Several planar transmission line structures can be used to make delay lines. Striplines are particularly suitable for delay line applications at microwave frequencies, offering nearly pure TEM propagation, a densely packaged structure, insignificant radiation loss, and minimized current crowding at the edges of the line.

In this system, all the delay lines are made with YBCO superconductor on 20-mil-thick $LaAlO_3$ substrates in dual spiral form [5]–[7]. The linewidth of all delay lines is 100 μm (with 45 Ω characteristic impedance) with tapered line transformers at both ends [8].

The key issues in delay line design include obtaining the desired impedance, maximizing line-to-line isolation, and making reflection free transitions from the stripline contact pad to other microstrip circuits. A stripline requires that the substrates be held in intimate contact with each other as the device is repeatedly cycled between room temperature and cryogenic temperatures. To insure phase reproducibility in a delay line structure which stores many wavelengths of analog signal, the residual air gap between the two substrates must be less than a fraction of a micrometer; otherwise, the change of impedance will cause severe reflection and generate microphonics due to mechanical vibration.

We have used a bed of beryllium-copper (BeCu) springs to press against the thin dielectric substrates and keep them in intimate contact with each other [9]–[10].

C. Cryogenic Mixers

By operating the mixers within the cryogenic enclosure, only one IF cable (with low thermal conductance) per discriminator is required, while two microwave cables (with higher thermal leakage) would be necessary if the mixers were at room temperature. At low operating temperature, the I-V curve of a Schottky diode is much steeper. This steep I-V curve creates a large current swing for a given voltage change. This increased nonlinearity makes possible low-power operation with low noise and low conversion loss. However, at low temperature the barrier height is increased, in turn increasing the required LO power for self biased operation. We use low-barrier height diodes to reduce the operating power level. The diode we used has a barrier height of 0.2 V. This type of

diode requires only 5–7 dBm LO power in a self-biased single balanced configuration for good mixer performance at low temperature.

Fig. 4 shows the measured I-V curve of a low-barrier diode at 77 K and 300 K, respectively. Fig. 5 is the layout of the mixer which is made with silver on a 25-mil-thick sapphire. As shown in Fig. 5, the LO signal is applied to a microstrip launcher and the RF signal is coupled to the diodes by two sections of quarter wave balun.

D. Power Divider

There are two types of power dividers used in this system. One is a five-way power divider feeding the discriminators and the others are the two-way power dividers within each discriminator. Both of them are made with silver on sapphire substrates. We utilize a standard Wilkinson power divider for two-way splitting. For the five-way power divider, we have modified the conventional power divider. The power dividers commonly used are the Wilkinson, radial, and planar structure [11]–[15]. The Wilkinson type has the advantage of low loss, moderate bandwidth, and good amplitude and phase balance. However, its major disadvantage is its nonplanar crossover configuration. The radial line divider has low loss, inherent phase symmetry, and good isolation, but it requires a three-dimensional structure [13]. The planar N-way combiner [14] requires $(N\text{-}1) \times N$ quarter wave sections for maximum isolation, and thus is very large in size. It also suffers on isolation, return loss and output power variation.

In order to make a power divider which has low loss, broad bandwidth, and good symmetry in a planar structure, we have modified a planar power divider structure. It has the combined advantages of the planar N-way combiner and the radial structure. Fig. 6 shows the layout of our power divider. We have added resistors R_a and R_b for more symmetry to increase the bandwidth and enhance the isolation. The high-impedance stub lines between resistors increase the isolation of the output channels. Calculations predict that the return loss of the input and all outputs are more than 20 dB, and the isolation is over 20 dB. The output power split is designed to be unequal to compensate for the insertion-loss difference in the different delay lines. At 4 GHz, the design output powers in this divider are −6.5 dB (port 3), −7.0 dB (ports 2 and 4), and −9.5 dB (ports 1 and 5).

One of the MSB channels requires a quadrature phase shift. We use a four-finger interdigital coupler (Lange coupler with four 48 μm wide fingers). In this structure the crossovers are implemented by wire bonding.

E. Room Temperature Postprocessor

The postprocessor has a fast differential comparator which can operate up to 30 MHz. The comparator output is designed to be five bit gray code, representing the instantaneous frequency of the input signal. The gray code is converted to binary code and then to decimal and is further displayed.

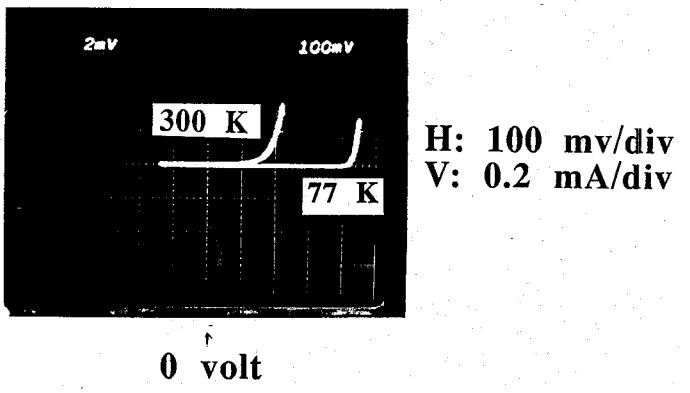

Fig. 4. I-V curve of a low-barrier height diode pair at 77 K and 300 K.

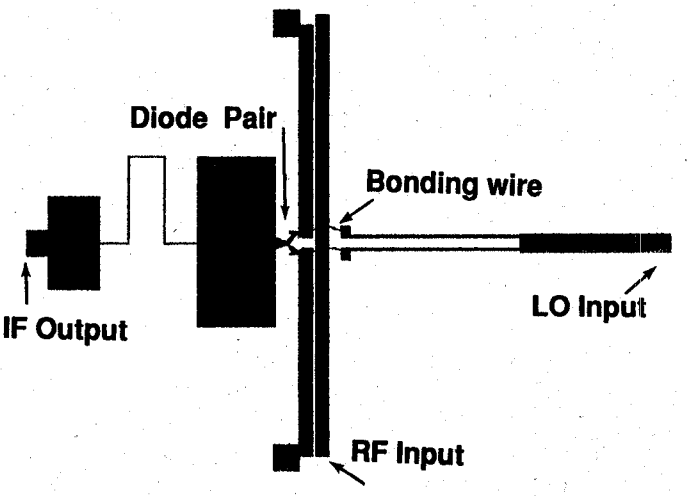

Fig. 5. Layout of the mixer.

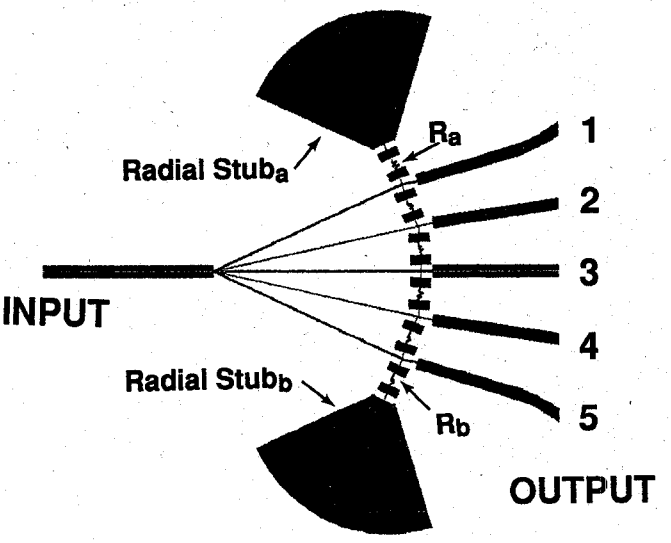

Fig. 6. Layout of a 5-way power divider.

F. Package

The overall package consists of six gold plated aluminum subpackages. Five of these are discriminator modules containing mixers and delay lines, which are a combination of stripline and microstrip line configurations.

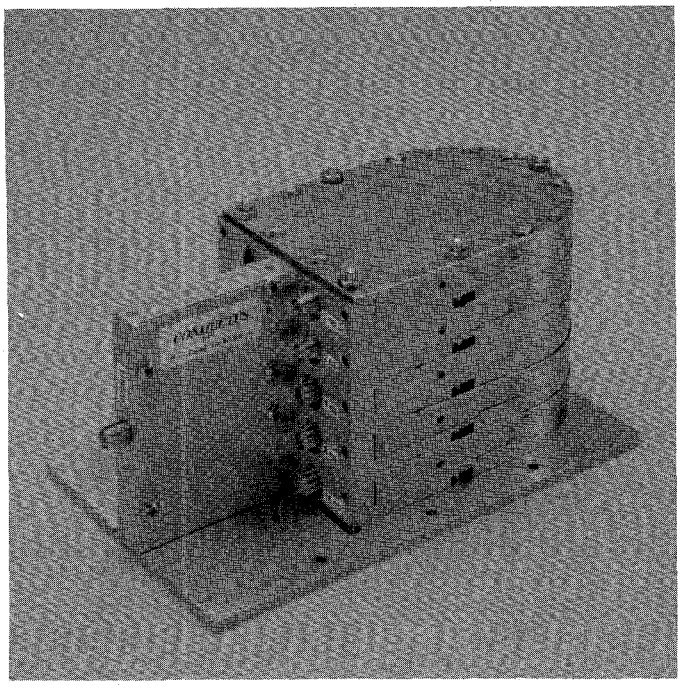

Fig. 7. Cryogenic section of DIFM system. The vertical section (bottom left) is the 5-way power divider. The five discriminator modules (top right) are stacked.

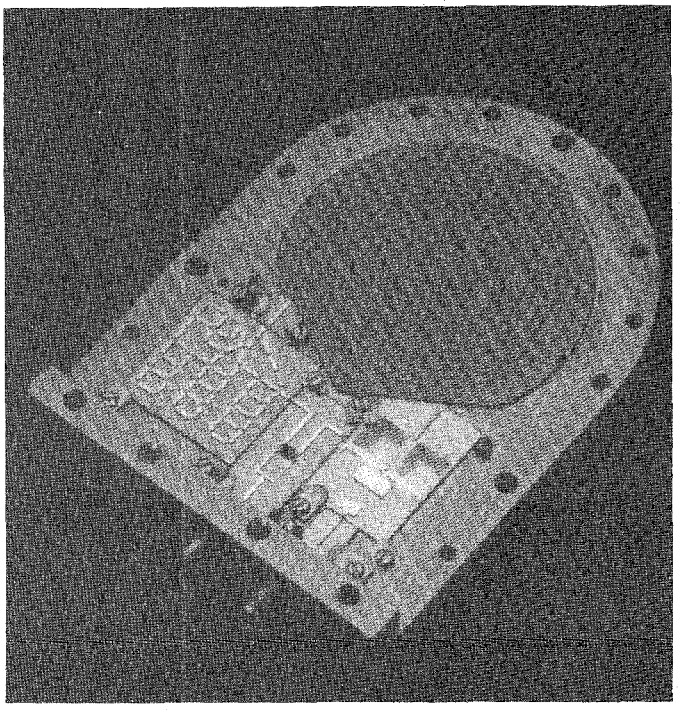

Fig. 8. Discriminator module with 16-ns delay line. The components are: bottom left—trimming delay line; bottom middle—a two-way power divider; bottom right—a self-biased mixer; upper right—a spiral delay line on $LaAlO_3$ substrate, with upper ground plane of the stripline removed to reveal the pattern.

The sixth subpackage contains the five way power divider in a microstrip configuration. These six subpackages are electrically connected by five "snap on" SMA connectors. Fig. 7 is a photograph of the assembled cryogenic section of the DIFM system. Fig. 8 shows a 16 ns discriminator module.

IV. Fabrication

YBCO films were made by the off-axis sputtering technique [16]–[17]. Patterning of the film was done by argon ion-beam etching, using standard positive photoresist. We have used sputtered silver and gold for bonding pads. For the normal metal circuits, we have used sputtered silver or gold on 25-mil-thick M plane sapphire, with a molybdenum adhesive layer. The metal films are also patterned by an ion-milling dry etch technique. Ground planes for the delay lines consist of either silver (for 2-, 4-, and 8-ns delay lines) or YBCO film (for the 16-ns delay line). The wire bonding is done with either an ultrasonic wire bonder or a gap welder using 5-mil-wide and 20-mil-wide ribbon.

V. Experimental Results and Discussion

We have fabricated and tested each part of the subsystem and evaluated the overall system performance. The performance of the components, modules, and complete IFM system is described below.

1) Delay Lines: Scattering parameters of these delay lines have not been measured outside of the discriminator modules. However, a comparable delay line, a 15.2 ns delay line on $LaAlO_3$ made at Conductus, has less than 3 dB insertion loss at 77 K at 6 GHz.

2) Mixers: The conversion loss versus frequency is shown in Fig. 9. At 4 GHz this was measured to be 7 dB at 77 K and 10 dB at 300 K. The variation is ± 0.75 dB within the 500 MHz bandwidth. In this measurement both LO and RF had a power level of 7.5 dBm. The LO/RF isolation is 18–22 dB, and the LO/IF isolation is over 40 dB.

3) Power dividers: The measured return loss for the two-way power divider is 15 dB. The insertion loss to both output ports is 3.1 ± 0.1 dB across the band. The five-way power divider shows a 16-dB return loss on the input port, 23- to 28-dB return loss on the outputs, and a 20- to 25-dB isolation between the outputs. The output power split at 300 K is -7.1 dB (port 3), -8.5 dB (ports 2 and 4), and -9.3 dB (ports 1 and 5).

4) One-Bit Discriminator Module: A delay trim network is used in conjunction with the delay line. Alternate paths through the Au/sapphire microstrip trim circuit are selected by wire bonding, so that the zero crossings of discriminator IF outputs occur at the design frequencies. The delay can be trimmed in units of 36 ps, and fine trimming can be made to 10 ps. Each comparator threshold value is also independently adjusted.

A superconductor has a penetration depth which is analogous to skin depth in normal metal. This penetration depth is not a function of frequency, but is temperature dependent. When the temperature goes down, the penetration depth will be reduced, and this will reduce the kinetic inductance, and, in turn, the amount of delay cre-

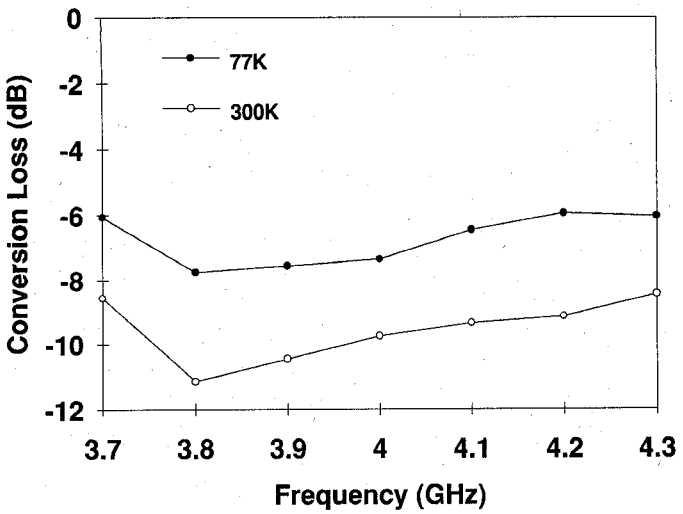

Fig. 9. Measured conversion loss of the mixer at 77 K and 300 K.

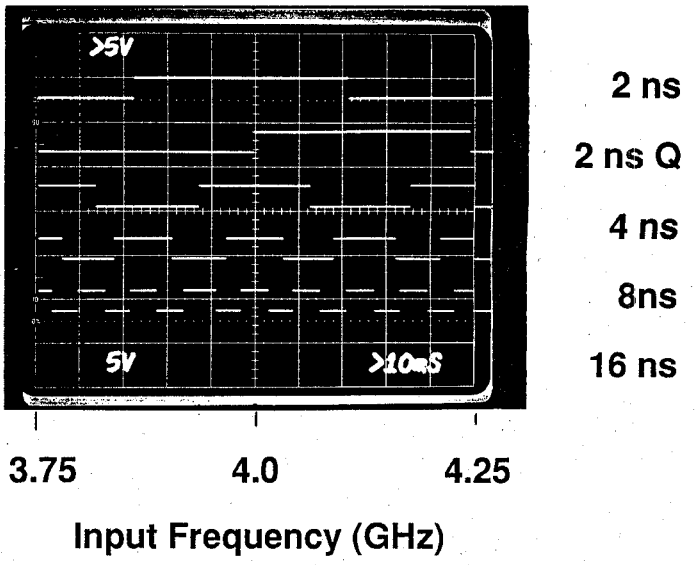

Fig. 12. The 5-bit digital output of the DIFM as a function of input frequency.

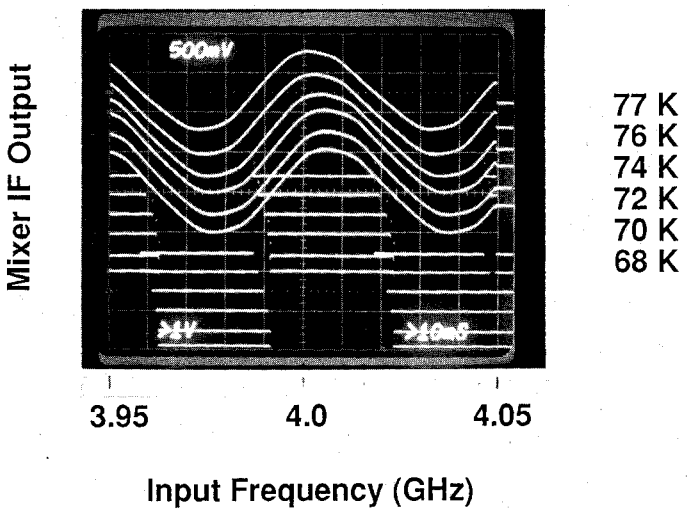

Fig. 10. IF output of a 16-ns discriminator versus operating temperature. The central 100 MHz of bandwidth is shown on an expanded scale.

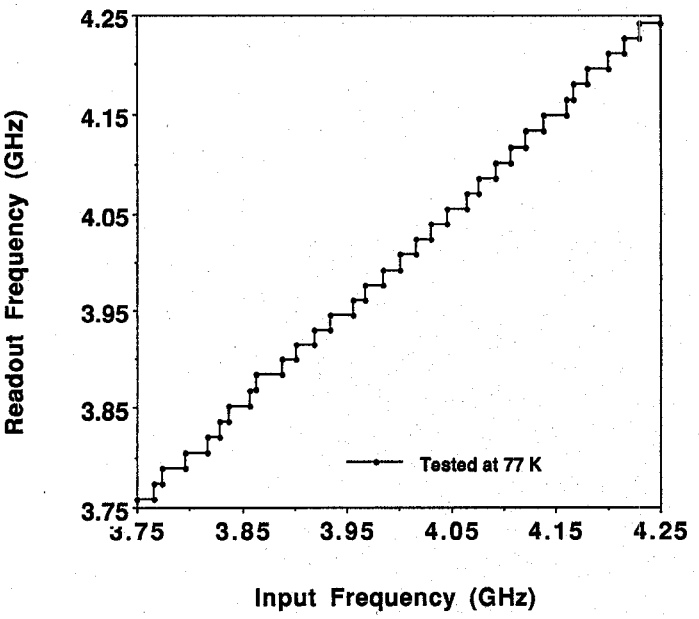

Fig. 13. DIFM frequency readout versus input frequency (CW test).

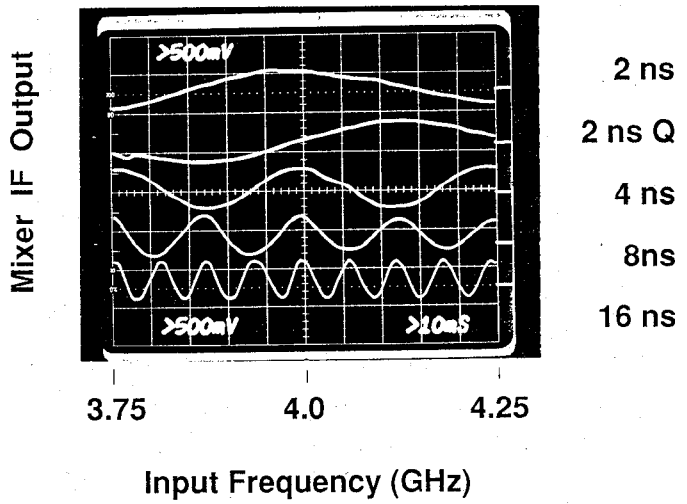

Fig. 11. The 5-bit analog output of the DIFM as a function of input frequency.

ated [18]. Fig. 10 shows the 16 ns discriminator IF output versus frequency (on an expanded scale) with different operating temperatures. As can be seen, the delay is stabilized when the temperature is below 74 K. The measurement is performed in liquid nitrogen. The lower temperature is realized by pumping on liquid nitrogen.

5) Complete System Test: The complete system has been tested in liquid nitrogen. Fig. 11 shows the output of the postprocessor unit, with a single swept input tone, as a function of the input frequency. The outputs of the 2-ns (in phase), 2-ns (quadrature), 4-, 8-, and 16-ns channels are arranged from top to bottom. Fig. 12 shows the digital output of the room temperature postprocessor corresponding to Fig. 11. Fig. 13 shows the frequency reported by the DIFM, under CW condition with a single

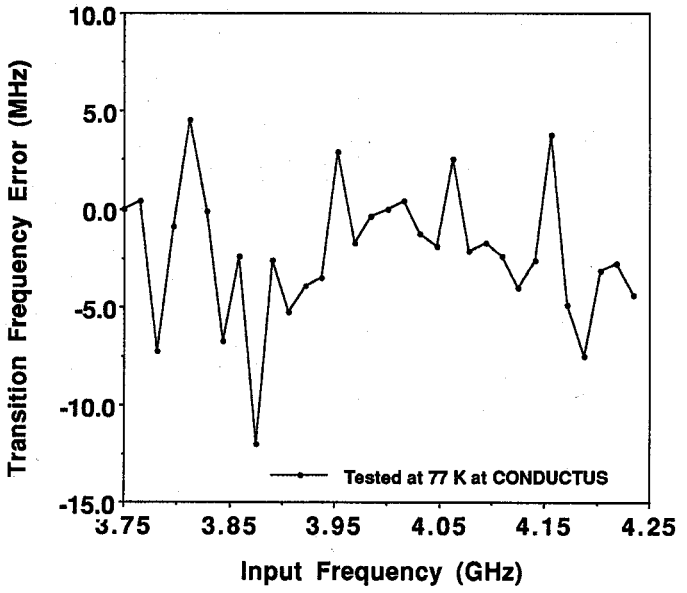

Fig. 14. Deviation of transition frequency from ideal value.

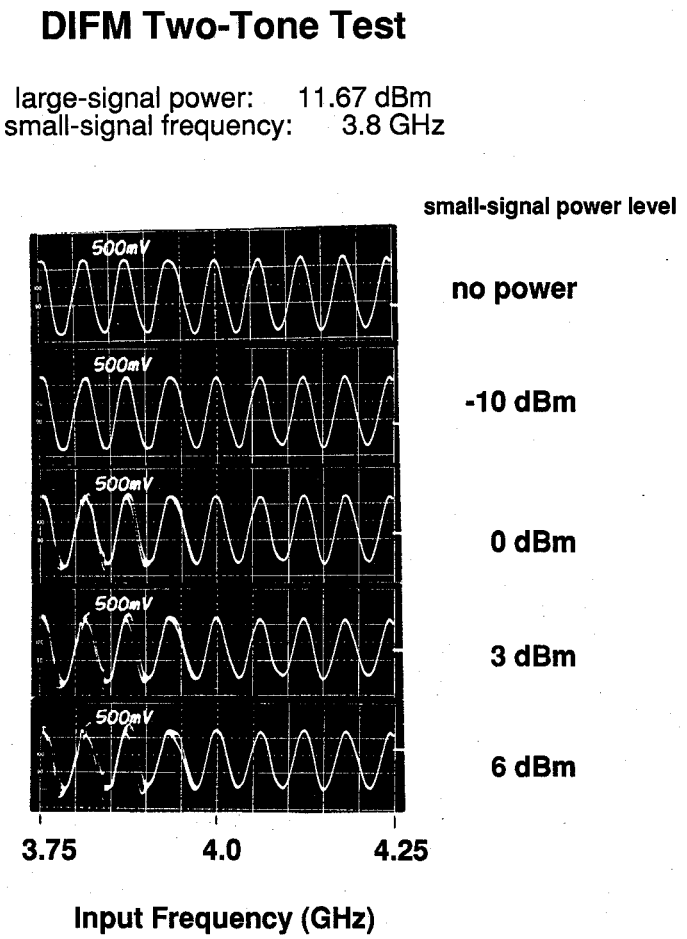

Fig. 15. IF output of a 16-ns discriminator, when two sources are applied at the same time. One is with a constant power of 11.7 dBm, sweeping over the band, while the other is tuned to 3.8 GHz and is of variable power. No limiting amplifier is used in testing.

stepped input tone, where the x-axis is the input frequency and the y-axis is the readout frequency indicated by the decoded binary signals shown in Fig. 12. Fig. 14 shows the deviation of the transition frequencies (that is, the frequencies at which the binary output changes) from the design values. The average of the magnitude of the error is 3.1 MHz. The input power dynamic range is between −40 dBm and +10 dBm.

We have also performed a dual-tone test without the limiting amplifier using two CW sources within the DIFM band. One source, with a constant power of 11.7 dBm, is sweeping over the band, while the other, weaker tone is tuned to 3.8 GHz. Fig. 15 shows the 16 ns discriminator output when two signals are present. The DIFM accurately reports the frequency of the stronger signal as long as the second signal is 10 dB lower. By using the limiting amplifier, the tolerable power difference can be 6 dB smaller because of its small signal suppression effect.

VI. Conclusion

We have reported a five bit superconductive digital instantaneous frequency measurement (DIFM) subsystem. The system has a center frequency of 4 GHz and a bandwidth of 500 MHz. The subsystem contains a cryogenic section with five discriminator modules utilizing superconductive delay lines, GaAs mixers, and power dividers. The subsystem also has a room-temperature GaAs limiting amplifier and a silicon postprocessor. With a single-tone CW input power between −40 dBm and +10 dBm, the frequency quantization boundaries of the subsystem are, on average, 3.1 MHz from their design values.

VII. Acknowledgment

The authors wish to thank M. Krivoruchko, S. Garrison, D. Zhang, and W. Ruby at Conductus for their assistance and consultation. They acknowledge the encouragement of J. Rowell, R. Simon, and B. Whalen.

References

[1] J. B.-Y. Tsui, *Microwave Receivers with Electronic Warfare Applications*. New York: Wiley, 1986.

[2] J. B.-Y. Tsui, *Microwave Receivers and Related Components*. Avionics Laboratory, Air Force Wright Aeronautical Laboratories, 1983.

[3] E. Wolff and R. Kaul, *Microwave Engineering and Systems Application*. New York: Wiley, 1988.

[4] R. Bauman, "Digital instantaneous frequency measurement for EW Receivers," *Microwave J.*, p. 147, Feb. 1985.

[5] G.-C. Liang, R. S. Withers, B. F. Cole, and N. Newman, "High-temperature superconductive devices on sapphire," presented at *1991 MTT Conf.*, to be published in *IEEE Trans. Microwave Theory Tech.*, Jan. 1994.

[6] G.-C. Liang, R. S. Withers, B. F. Cole, S. M. Garrison, M. E. Johansson, W. Ruby, and W. G. Lyons, "High-temperature superconducting delay lines and filters on sapphire and thinned $LaAlO_3$ substrates," vol. 3, pp. 3037-3042, *IEEE Trans. Appl. Superconductivity*, Sept. 1993.

[7] W. G. Lyons, R. S. Withers, J. M. Hamm, A. C. Anderson, P. M. Mankiewich, M. L. O'Malley, and R. E. Howard, "High-Tc superconductive delay line structures and signal conditioning networks," *IEEE Trans. Magnetics*, vol. 27, pp. 2932-2935, March 1991.

[8] R. W. Klopfenstein, "A transition line taper of improved design," *Proc. IRE*, pp. 31-35, 1956.

[9] A. C. Anderson, R. S. Withers, S. A. Reible, and R. W. Ralston, "Substrates for superconductive analog signal processing devices," *IEEE Trans. Magnetics*, vol. 19, pp. 485-489, May 1983.

[10] R. S. Withers, A. C. Anderson, J. B. Green, and S. A. Reible, "Superconductive delay line technology and applications," *IEEE Trans. Magnetics*, vol. 21, pp. 186–192, March 1985.
[11] E. Wilkinson, "An n-way hybrid power divider," *IRE Trans. Microwave Theory Tech.*, vol. 8, pp. 116–118, Jan. 1960.
[12] W. Yau and J. M. Schellenberg, "An n-way broadband planar power combiner/divider," *Microwave J.*, vol. 29, pp. 147–151, Nov. 1986.
[13] J. M. Schellenberg and M. Cohn, "A wideband radial power combiner for FET amplifier," *IEEE Int. Solid State Circuits Conf. Dig.*, pp. 164–168, Feb. 1978.
[14] A. A. M. Saleh, "Planar electrically symmetric n-way hybrid power divider/combiners," *IEEE Trans. Microwave Theory Tech.*, vol. 28, pp. 555–563, June 1984.
[15] N. Nagai, E. Mackawa, and K. Ono, "New n-way hybrid power dividers," *IEEE Trans. Microwave Theory Tech.*, vol. 25, pp. 1008–1012, Dec. 1977.
[16] N. Newman, K. Char, S. M. Garrison, R. W. Barton, R. C. Taber, C. B. Eom, T. H. Geballe, and B. Wilkens, "$YBa_2Cu_3O_{7-\delta}$ superconducting films with low microwave surface resistance over large areas," *Appl. Phys. Lett.*, vol. 57, pp. 520–522, May 1990.
[17] B. F. Cole, G.-C. Liang, K. Char, G. Zaharchuk, and J. S. Martens, "Large-area YBCO films on sapphire for microwave applications," *Appl. Phys. Lett.*, vol. 61, pp. 1727–1729, Oct. 1992.
[18] T. Van Duzer and C. W. Turner, *Principles of Superconductive Devices and Circuits*. New York: Elsevier, 1981.

Guo-chun Liang (S'87–M'90) was born in Jiangsu, People's Republic of China. He received the B.S. degree in electrical engineering from the East China Institute of Technology, Naijing, China, in 1982, the M.S. degree in electrical engineering from the University of Electronics, Science, and Technology of China (UEST), Chengdu, China, in 1985, and the Ph.D. degree from the Department of Electrical Engineering and Computer Science, University of California at Berkeley, in 1990.

He was with the Microwave Center of UEST in 1985 and 1986. Currently, he is with Conductus, Inc., Sunnyvale, California. He has been actively involved in research and development of various superconductive rf and microwave circuits and systems, including resonators, filters, mixers, delay lines, phase shifters, instantaneous frequency measurement system (High-Temperature Superconductor Space Experiment Program, Phase II) and magnetic resonance imaging coils. His interests include superconductor electronics and their applications, microwave circuits and systems, mobile cellular telecommunications systems, and numerical analysis and simulation of electromagnetic problems.

Chien-Fu Shih received the B.S. degree in physics from Fu-Jen University, Taiwan, in 1970, the M.S. degree in physics from the University of Wisconsin, Superior, in 1972, and the M.S.E.E. degree from Oregon State University, Corvalis, in 1978.

From 1978 to 1981, he worked as a Microwave Engineer at Addington Laboratory, Eaton Corporation. During that period, he worked on microwave voltage controlled oscillators and multipliers. Later, he worked as an Integration Engineer at Ford Aerospace Corporation, designing the transponder circuit. In 1984, he joined Hewlett Packard Company as an engineer, designing the spectrum analyzer. In 1992, he joined Conductus, Inc. Since then he has been involved in the design and measurement of superconductive digital instantaneous frequency measurement subsystem, resonators, and filters.

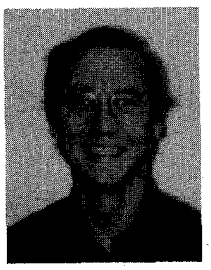

Richard S. Withers received the S.B., S.M., and Sc.D. degrees in electrical engineering from the Massachusetts Institute of Technology, in 1976, 1976, and 1978, respectively.

From 1978–1984, he was a member of the Technical Staff at M.I.T. Lincoln Laboratory. During this time, he developed niobium tapped delay lines, silicon charge-coupled devices, and surface-acoustic wave devices. Until 1991, he was Associate Leader of the Analog Device Technology Group at M.I.T. Lincoln Laboratory. In that capacity, he directed Lincoln's development of microwave circuits using high-temperature superconductor, including its delivery of space-qualified filters for the Navy's HTSSE-I program. In 1991, he joined Conductus, Inc., Sunnyvale, CA, where he is the Head of Analog System Development. Until 1992, he was the program manager for microwave networks within the Consortium for Superconducting Electronics, and in that capacity, coordinated efforts at Conductus, Lincoln Laboratory, IBM, AT&T Bell Laboratory, M.I.T., Cornell University, and Boston University. His interests are in microwave and RF applications of superconductivity, in such fields as communications, instrumentation, and medical imaging.

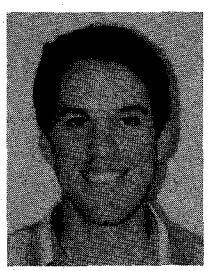

Brady F. Cole received the B.S. degree in ceramic science and engineering from the Pennsylvania State University in 1988.

Since joining Conductus in 1989, he has investigated the growth of high-T_c superconducting thin films. He has developed methods of depositing high quality films on large area sapphire substrates, and has established large-scale production of films with low-microwave surface resistance. His current professional interests include high-T_c multilayer films and microstructure-transport property relationships.

Marie E. Johansson received the B.S. degree in physics from the University of Linköping, Sweden, 1986.

From 1986 to 1989, she designed and produced passive microwave devices at the National Defense Research Institute in Linköping, Sweden. She then developed process techniques for high-T_c thin films at the National Institute of Standards and Technology, Boulder, CO. Since joining Conductus, Inc., in June 1992, she has been working on the development and processing of high-T_c superconducting microwave and digital devices.

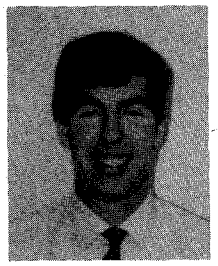

Larry P. Suppan, Jr. received the B.S. degree in electronics engineering from California Polytechnic State University in 1990.

He was with Applied Navigation devices where he was responsible for the design change of an inverter system used to run a gyro in a bore hole navigation tool. Currently, he is with Conductus, Inc., where he is involved in the design and manufacture of prototype electronic instrumentation for SQUID and bolometer applications.